

## Plaquette Ordered Phase and Quantum Phase Diagram in the Spin- $\frac{1}{2}$ $J_1$ - $J_2$ Square Heisenberg Model

Shou-Shu Gong,<sup>1</sup> Wei Zhu,<sup>1</sup> D. N. Sheng,<sup>1</sup> Olexei I. Motrunich,<sup>2</sup> and Matthew P. A. Fisher<sup>3</sup>

<sup>1</sup>*Department of Physics and Astronomy, California State University, Northridge, California 91330, USA*

<sup>2</sup>*Department of Physics, California Institute of Technology, Pasadena, California 91125, USA*

<sup>3</sup>*Department of Physics, University of California, Santa Barbara, California 93106-9530, USA*

(Received 8 February 2014; revised manuscript received 7 May 2014; published 7 July 2014)

We study the spin-1/2 Heisenberg model on the square lattice with first- and second-neighbor antiferromagnetic interactions  $J_1$  and  $J_2$ , which possesses a nonmagnetic region that has been debated for many years and might realize the interesting  $Z_2$  spin liquid. We use the density matrix renormalization group approach with explicit implementation of  $SU(2)$  spin rotation symmetry and study the model accurately on open cylinders with different boundary conditions. With increasing  $J_2$ , we find a Néel phase and a plaquette valence-bond (PVB) phase with a finite spin gap. From the finite-size scaling of the magnetic order parameter, we estimate that the Néel order vanishes at  $J_2/J_1 \approx 0.44$ . For  $0.5 < J_2/J_1 < 0.61$ , we find dimer correlations and PVB textures whose decay lengths grow strongly with increasing system width, consistent with a long-range PVB order in the two-dimensional limit. The dimer-dimer correlations reveal the  $s$ -wave character of the PVB order. For  $0.44 < J_2/J_1 < 0.5$ , spin order, dimer order, and spin gap are small on finite-size systems, which is consistent with a near-critical behavior. The critical exponents obtained from the finite-size spin and dimer correlations could be compatible with the deconfined criticality in this small region. We compare and contrast our results with earlier numerical studies.

DOI: 10.1103/PhysRevLett.113.027201

PACS numbers: 75.10.Jm, 75.10.Kt

*Introduction.*—Quantum spin liquid (SL) is an exotic state of matter where a spin system does not form a magnetically ordered state or break lattice symmetries even at zero temperature [1]. Understanding spin liquids is important in frustrated magnetic systems and may also hold clues to understanding the non-Fermi liquid of doped Mott materials and high- $T_c$  superconductivity [2]. While the exciting properties of SL such as deconfined quasiparticles and fractional statistics have been revealed in many artificially constructed systems [3–12], the possibility of finding spin liquids in realistic Heisenberg models has attracted much attention over the past 20 years due to its close relation to experimental materials. The prominent example is the kagome antiferromagnet, where recent density matrix renormalization group (DMRG) studies point to a gapped  $Z_2$  SL [10,13–16] characterized by a  $Z_2$  topological order and fractionalized spinon and vison excitations [17–21].

One of the candidate models for SL is the spin- $\frac{1}{2}$   $J_1$ - $J_2$  square Heisenberg model (SHM) with the Hamiltonian

$$H = J_1 \sum_{\langle i,j \rangle} S_i \cdot S_j + J_2 \sum_{\langle\langle i,j \rangle\rangle} S_i \cdot S_j, \quad (1)$$

where the sums  $\langle i,j \rangle$  and  $\langle\langle i,j \rangle\rangle$  run over all the nearest-neighbor (NN) and the next-nearest-neighbor bonds, respectively. We set  $J_1 = 1$ . The frustrating  $J_2$  couplings suppress the Néel order and induce a nonmagnetic region around the strongest frustration point  $J_2 = 0.5$  [22–47]. Different candidate states have been proposed based on approximate methods or small-size exact diagonalization calculations,

such as the plaquette valence-bond (PVB) state [26,29,32,33,35,38,46], the columnar valence-bond (CVB) state [24,25,28], or a gapless SL [30,31,44,45]. However, the true nature of the nonmagnetic phase remains unresolved.

Recent DMRG study of the  $J_1$ - $J_2$  SHM [40] proposed a gapped  $Z_2$  SL for  $0.41 \leq J_2 \leq 0.62$  by establishing the absence of the magnetic and dimer orders, and by measuring a positive topological entanglement entropy term close to the value  $\ln 2$  expected for a  $Z_2$  SL [48,49]. Very recent variational Monte Carlo work [45] proposed a gapless  $Z_2$  SL for  $0.45 \lesssim J_2 \lesssim 0.6$ . On the other hand, recent DMRG studies [50–52] of another bipartite frustrated system—the  $J_1$ - $J_2$  spin-1/2 honeycomb Heisenberg model—found a PVB phase in the nonmagnetic region, with a possible SL phase between the Néel and PVB phases [52] or with a direct Néel-to-PVB transition characterized by deconfined quantum criticality [50–54]. These studies [51,52] also found that in the nonmagnetic region the convergence of DMRG in wider systems, which is controlled by the number of states kept, is crucial for determining the true nature of the ground state.

In this Letter, we reexamine the nonmagnetic region of the  $J_1$ - $J_2$  SHM using DMRG with  $SU(2)$  spin rotation symmetry [55]. We obtain accurate results on wide cylinders by keeping as many as 36000  $U(1)$ -equivalent states. We find a Néel phase below  $J_2 \approx 0.44$  and a nonmagnetic region for  $0.44 < J_2 < 0.61$  by finite-size scaling of the magnetic order parameter. In the nonmagnetic region, we establish a PVB order for  $J_2 > 0.5$ —in contrast to the previous proposal of a

gapped  $Z_2$  SL [40]—by observing that the PVB decay length grows strongly with increasing system width. We identify the PVB order as the  $s$ -wave plaquette [33] by studying dimer-dimer correlations. For  $0.44 < J_2 < 0.5$ , we find that the magnetic order, valence-bond crystal (VBC) orders, and spin excitation gap are small on finite-size systems, suggesting a near-critical behavior. The magnetic and dimer critical exponents at  $J_2 = 0.5$  are roughly similar to the values found for the deconfined criticality in the  $J$ - $Q$  models on the square and honeycomb lattices [56–63], which is consistent with the deconfined criticality scenario conjectured also for the  $J_1$ - $J_2$  model in Ref. [64].

We establish the phases based on high accuracy DMRG results on cylinders [65]. The first cylinder is the rectangular cylinder (RC) with closed boundary in the  $y$  direction and open boundaries in the  $x$  direction. We denote it as  $\text{RCL}_y\text{-}L_x$ , where  $L_y$  and  $L_x$  are the number of sites in the  $y$  and  $x$  directions; the width of the cylinder is  $W_y = L_y$  (see the inset of Fig. 1). To study the dimers oriented in the  $y$  direction, we can induce such an order near the open boundaries by modifying every other NN vertical bond on the boundary to be  $J_{\text{pin}} \neq J_1$  as illustrated in Fig. 1. The second geometry is the tilted cylinder (TC), as shown in Fig. 4(a), when discussing VBC order.

*Néel order.*—The Néel order parameter  $m_s^2$  is defined as  $m_s^2 = \frac{1}{N^2} \sum_{i,j} \langle S_i \cdot S_j \rangle e^{i\vec{q} \cdot (\vec{r}_i - \vec{r}_j)}$  ( $N$  is the total site number), with  $\vec{q} = (\pi, \pi)$ . We calculate  $m_s^2$  from the spin correlations of the  $L \times L$  sites in the middle of the  $\text{RCL-}2L$  cylinder, which efficiently reduces boundary effects [40,66]. In Fig. 2(a), we show  $m_s^2$  for different systems with  $L = 4\text{--}14$  [67]. We show the obtained two-dimensional limit  $m_{s,\infty}^2$  in

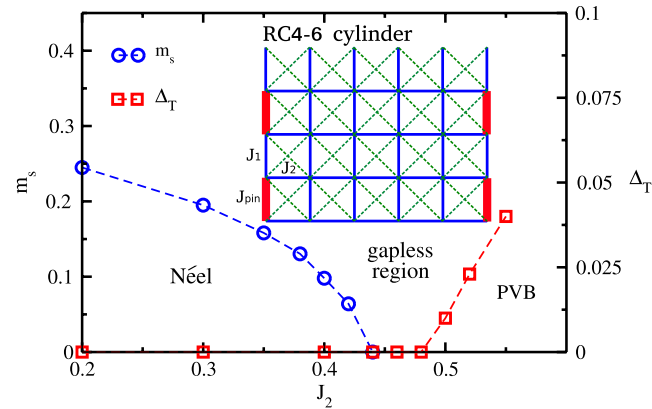


FIG. 1 (color online). Phase diagram of spin-1/2  $J_1$ - $J_2$  SHM obtained by our  $SU(2)$  DMRG studies. With growing  $J_2$ , the model has a Néel phase for  $J_2 < 0.44$  and a PVB phase for  $0.5 < J_2 < 0.61$ . Between these two phases, the finite-size magnetization and spin gap appear small in our calculations, consistent with a near-critical behavior. The main panel shows Néel order parameter  $m_s$  and spin gap  $\Delta_T$  in the thermodynamic limit. The inset is a sketch of a RC4-6 cylinder;  $J_{\text{pin}}$  shows the modified odd vertical bonds providing the boundary pinning for dimer orders.

the inset of Fig. 2(a). Such an analysis suggests that the Néel order vanishes for  $J_2 > 0.44$ .

The estimated  $J_2$  of spin order vanishing is different from the point  $J_2 = 0.5$  where the PVB order develops as found below. One possibility is an intermediate SL phase [44,45]. Another possibility is that the system is near critical for  $0.44 < J_2 < 0.5$ . In this case, to get some idea about the criticality, Fig. 2(b) shows the log-log plot of  $m_s^2(L)$ .  $m_s^2$  approaches finite value in the Néel phase as seen for  $J_2 = 0.35$  and  $0.4$ . On the other hand, we expect  $m_s^2(L) \sim L^{-(1+\eta)}$  at a critical point and  $m_s^2(L) \sim L^{-2}$  in the nonmagnetic phase. The accelerated decay of  $m_s^2(L)$  at  $J_2 = 0.55$  is consistent with vanishing Néel order: from the two largest sizes we estimate  $m_s^2(L) \sim L^{-1.82}$ , which is quite close to  $m_s^2(L) \sim L^{-2}$ . In the near-critical region, we fit the  $J_2 = 0.44$  data to  $L^{-(1+0.15)}$  and the  $J_2 = 0.5$  data ( $L > 8$ ) to  $L^{-(1+0.44)}$ . This range of  $\eta$  is compatible with the findings in the  $J$ - $Q$  models on the square ( $\eta \approx 0.26\text{--}0.35$ ) [56–62] and honeycomb ( $\eta \approx 0.3$ ) [63] lattices, which show continuous Néel-to-VBC transition argued to be in the deconfined criticality class, so our model is compatible with this scenario as well.

*VBC orders.*—We introduce the “pinning” bonds  $J_{\text{pin}} \neq J_1$  on boundaries to induce a vertical dimer pattern and

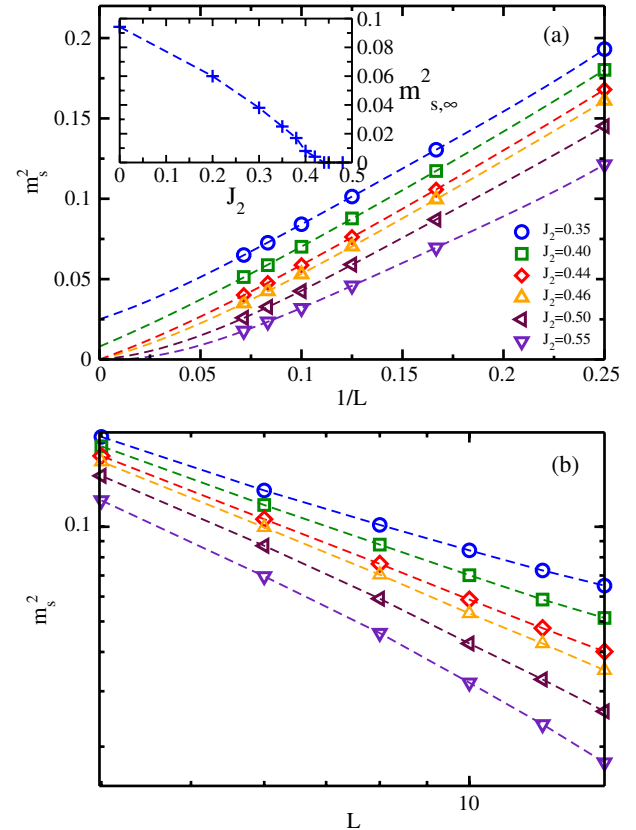


FIG. 2 (color online). (a)  $m_s^2$  plotted versus  $1/L$  for  $\text{RCL-}2L$  cylinder with  $L = 4, 6, 8, 10, 12, 14$ ; lines are polynomial fits up to fourth order. The inset is  $J_2$  dependence of the obtained magnetic order in the 2D limit  $m_{s,\infty}^2$ . (b) Same data as (a) shown as log-log plot of  $m_s^2$  versus width  $L$ .

measure the decay length of the dimer order parameter (DOP) texture from the edge to the middle of the cylinder [40,64]. The vertical DOP (vDOP) is defined as the difference between the strong and weak vertical bond energies. In Fig. 3(a), we show a log-linear plot of the vDOP for  $J_2 = 0.5$  and  $J_{\text{pin}} = 2.0$  on long cylinders. We find that, although the amplitude of the vDOP texture changes with  $J_{\text{pin}}$ , the decay length  $\xi_y$  is independent of  $J_{\text{pin}}$

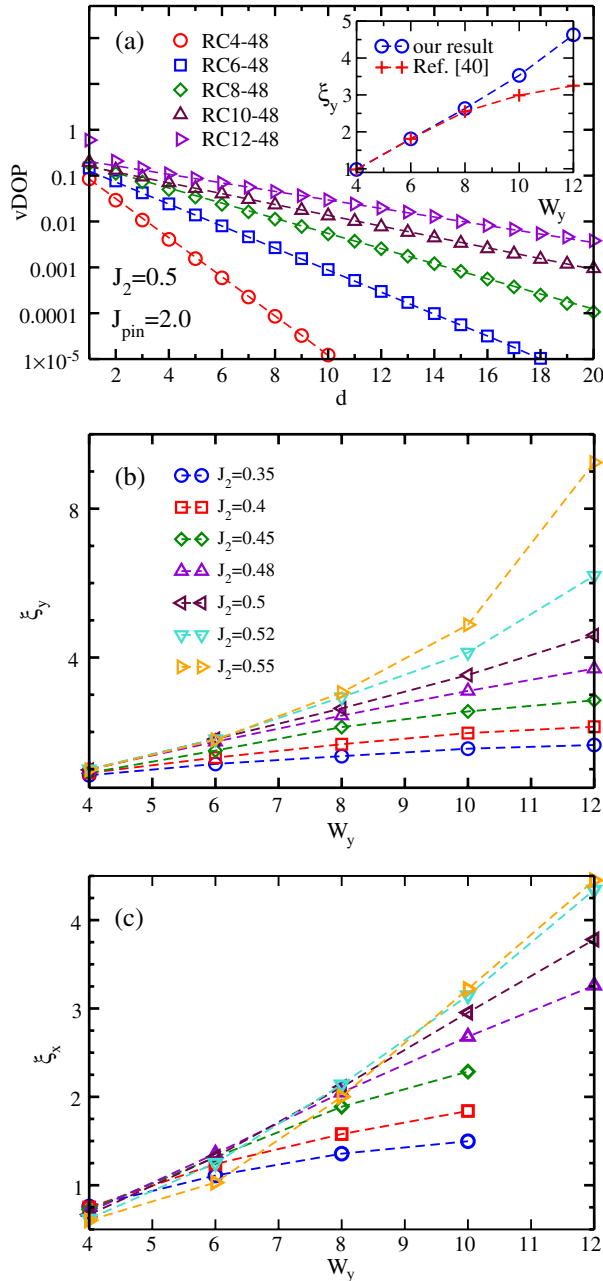


FIG. 3 (color online). (a) Log-linear plot of vDOP for  $J_2 = 0.5$  and  $J_{\text{pin}} = 2.0$  on the RC cylinder. The inset is the comparison of width dependence of the vertical dimer decay length  $\xi_y$  with Ref. [40]. (b),(c)  $\xi_y$  and  $\xi_x$  versus  $W_y$  on RC cylinders with  $J_{\text{pin}} = 2.0$  for a range of  $J_2$  shown with the same symbols in both panels.

(see Supplemental Material [68]). In the inset of Fig. 3(a) we compare our  $\xi_y$  with those in Ref. [40]. We observe consistency for  $W_y \leq 8$ , but disagreement for  $W_y \geq 10$  [69]. The disagreement might originate from less good convergence in Ref. [40]. Our results are fully converged by keeping 16 000 (24 000) states for  $L_y = 10$  (12) systems. In Fig. 3(b), we show the width dependence of  $\xi_y$  for various  $J_2$ .  $\xi_y$  grows slowly and saturates on wide cylinders for  $J_2 < 0.5$ , demonstrating the vanishing VBC order. For  $J_2 > 0.5$ ,  $\xi_y$  grows faster than linear, suggesting nonzero vDOP in the 2D limit. In addition to the vertical dimer, the system also has the horizontal bond dimer with an exponentially decaying horizontal DOP (hDOP). In Fig. 3(c), we show that the hDOP decay length  $\xi_x$  also grows strongly for  $J_2 > 0.5$ . The coexisting nonzero horizontal and vertical dimer orders suggest a PVB state.

We also study the dimer structure factors  $S_{\text{VBC}}$  and  $S_{\text{col}}$  defined in Ref. [33]; the former detects both the PVB and CVB orders while the latter is nonzero only for the CVB order. We take RCL- $2L$  cylinders without pinning and calculate the structure factors using the dimer correlations of the middle  $L \times L$  sites. The picture of the dimer correlations is consistent with the  $s$ -wave plaquette state [33]. The finite-size extrapolations show that while  $S_{\text{VBC}}/N$  possibly approaches finite values for  $J_2 > 0.5$ ,  $S_{\text{col}}/N$  clearly approaches zero, which definitely excludes the CVB order.

To explicitly demonstrate PVB order, we study the TC obtained by cutting the cylinder along the  $J_2$  direction and trimming every other site on the boundary as shown in Fig. 4(a). We label it as TCL $_y$ - $L_x$ , where  $L_y$  and  $L_x$  denote the number of square plaquettes along the  $y$  and  $x$  directions; the width of the cylinder is  $W_y = \sqrt{2}L_y$ . The trimmed edges induce strong PVB order on the boundaries. We denote the sum of the four NN bond energies of a “strong” red (“weak” blue) plaquette as  $E_s$  ( $E_w$ ) and define the plaquette DOP (pDOP) as the difference between  $E_s$  and  $E_w$ , which is found to decay exponentially with a decay length  $\xi_p$ . In Fig. 4(b), we find strong growth of  $\xi_p$  with  $W_y$  for  $J_2 > 0.5$ , consistent with a PVB state. By studying the log-log plot of the VBC order parameter versus system size (see Supplemental Material [68]), we estimate the anomalous exponent of dimer correlations  $\eta_{\text{VBC}} \approx 0.4$  at  $J_2 = 0.5$ , which is not far from estimates in the deconfined criticality scenario in the  $J$ - $Q$  models on square ( $\eta_{\text{VBC}} \approx 0.25$ ) [56–62] and honeycomb ( $\eta_{\text{VBC}} \approx 0.28$ ) [63] lattices.

*Spin gap and ground-state energy.*—We calculate the spin gap  $\Delta_T$  on the RCL- $2L$  cylinders up to  $L = 10$  following the method from Ref. [14]: We sweep the ground state first, and then target the  $S = 1$  sector sweeping the middle  $L \times L$  sites to avoid edge excitations. In Figs. 5(a) and 5(b), we show energies versus the DMRG truncation error for the RC10-20 cylinder at  $J_2 = 0.5$  in the  $S = 0$  and  $S = 1$  sectors. In both plots we have subtracted the ground-state energy  $-99.022(1)$  obtained by the extrapolation in Fig. 5(a). We find that we need about twice as many states

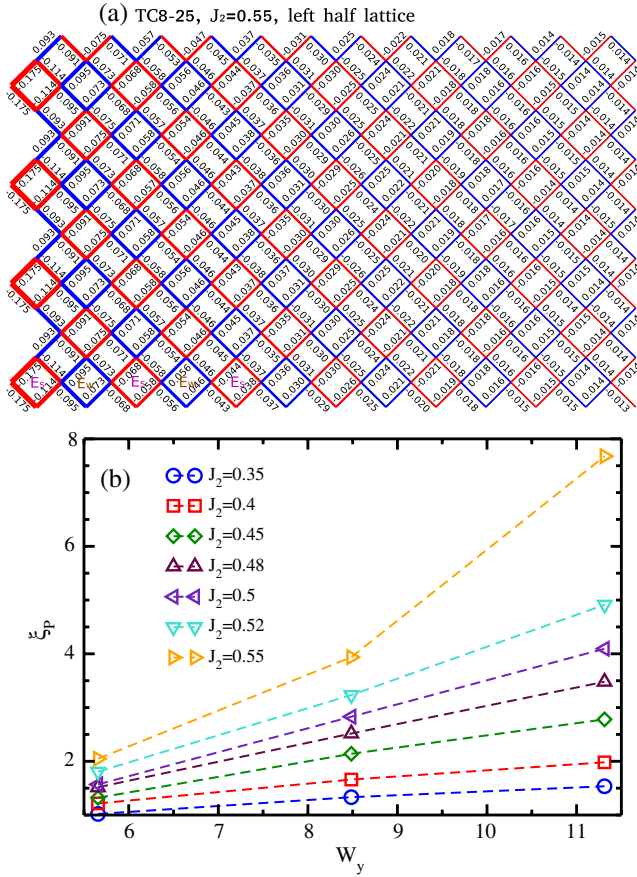


FIG. 4 (color online). (a) The NN  $J_1$  bond energy for  $J_2 = 0.55$  on the left half of the tilted TC8-25 cylinder, where we have subtracted a constant  $-0.2948$  from all the bond energies. Note that the TC cylinders have the square lattice rotated by  $45^\circ$  compared to Fig. 1. We trim every other site on both boundaries to make lattice select unique PVB order.  $E_s$  ( $E_w$ ) denotes the sum of four NN bond energies of the red (blue) plaquette with negative (positive) numbers. (b) Dependence of the pDOP decay length  $\xi_P$  on the cylinder width  $W_y$ .

to achieve the same energy error in the  $S = 1$  sector as in the  $S = 0$  sector. The difficulty to reach the convergent energy in the  $S = 1$  sector may explain the overestimate of the spin gap in the earlier work [40]: We find  $\Delta_T \approx 0.207$  while Ref. [40] estimates  $\Delta_T \approx 0.248$ . We obtain accurate spin gaps by keeping up to 36000 states at  $L_y = 10$ , which sets the limit of our simulations.

Figure 5(c) shows the finite-size extrapolations of  $\Delta_T$ . In our fits, we find  $\Delta_T$  extrapolating vanishing for  $J_2 \leq 0.48$ , consistent with the Néel order for  $J_2 \leq 0.44$ . For  $J_2 = 0.5$  and  $0.55$ ,  $\Delta_T(L \rightarrow \infty)$  is fitted to  $0.018 \pm 0.01$  and  $0.04 \pm 0.01$ , respectively; this is compatible with a VBC phase.

*Summary and discussion.*—We have studied the ground state of spin-1/2  $J_1$ - $J_2$  SHM by accurate  $SU(2)$  DMRG simulations. We find a Néel order persisting up to  $J_2 = 0.44$ . Contrary to the previous proposals of gapped  $Z_2$  SL from DMRG [40] or gapless  $Z_2$  SL from variational Monte Carlo

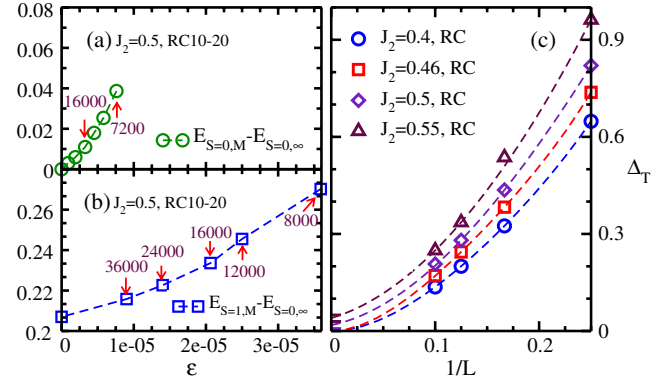


FIG. 5 (color online). (a),(b) Ground-state energies for RC10-20 cylinder at  $J_2 = 0.5$  in the  $S = 0$  ( $E_{S=0,M}$ ) and  $S = 1$  ( $E_{S=1,M}$ ) sectors versus the DMRG truncation error  $\epsilon$ . All the energies have subtracted the ground-state energy  $E_{S=0,\infty} = -99.022(1)$ .  $M$  is the number of kept  $U(1)$ -equivalent DMRG states and is indicated next to the symbols. (c) Finite-size extrapolations of spin gap  $\Delta_T$  on RCL-2L cylinders ( $L = 4, 6, 8, 10$ ). For  $J_2 < 0.5$ , the data are fitted using the formula  $\Delta_T(L) = \Delta_T(\infty) + \alpha/L^2 + \beta/L^3 + \gamma/L^4$ , while for  $J_2 \geq 0.5$ , we fit the data using  $\Delta_T(L) = \Delta_T(\infty) + a/L + b/L^2 + c/L^4$ . We estimate  $\Delta_T(\infty) = 0.018 \pm 0.01$  and  $0.04 \pm 0.01$  for  $J_2 = 0.5$  and  $0.55$ , respectively.

calculations [45], we establish an  $s$ -wave PVB state for  $J_2 > 0.5$  by observing rapidly growing characteristic lengths of both the vertical and horizontal dimer orders on different cylinders. Between the Néel and PVB phases, we find a near-critical region that could be compatible with the deconfined criticality scenario. However, since the system in this region has large correlation length scales that can be comparable to or even larger than the system widths we can approach, we cannot exclude a possible gapless SL region proposed in variational studies [44,45]. We hope that future studies on a larger system size, either pushing DMRG further or using new techniques such as tensor network, will be able to resolve between these scenarios more clearly.

We would like to particularly thank H.-C. Jiang and L. Balents for extensive discussions. We also acknowledge stimulating discussions with K. S. D. Beach, Z.-C. Gu, W.-J. Hu, L. Wang, S. White, Z.-Y. Zhu, and A. Sandvik. This research is supported by the National Science Foundation through Grants No. DMR-1205734 (S.-S. G.), No. DMR-0906816 (D. N. S.), No. DMR-1206096 (O. I. M.), No. DMR-1101912 (M. P. A. F.), the U.S. Department of Energy, Office of Basic Energy Sciences under Grant No. DE-FG02-06ER46305 (W. Z.), and the Caltech Institute of Quantum Information and Matter, a NSF Physics Frontiers Center with support of the Gordon and Betty Moore Foundation (O. I. M. and M. P. A. F.).

[1] L. Balents, *Nature (London)* **464**, 199 (2010).

[2] P. A. Lee, N. Nagaosa, and X. G. Wen, *Rev. Mod. Phys.* **78**, 17 (2006).

- [3] R. Moessner and S. L. Sondhi, *Phys. Rev. Lett.* **86**, 1881 (2001).
- [4] C. Nayak and K. Shtengel, *Phys. Rev. B* **64**, 064422 (2001).
- [5] T. Senthil and O. Motrunich, *Phys. Rev. B* **66**, 205104 (2002).
- [6] L. Balents, M. P. A. Fisher, and S. M. Girvin, *Phys. Rev. B* **65**, 224412 (2002).
- [7] D. N. Sheng and L. Balents, *Phys. Rev. Lett.* **94**, 146805 (2005).
- [8] S. V. Isakov, Y. B. Kim, and A. Paramekanti, *Phys. Rev. Lett.* **97**, 207204 (2006).
- [9] S. V. Isakov, M. B. Hastings, and R. G. Melko, *Nat. Phys.* **7**, 772 (2011).
- [10] Y. C. He, D. N. Sheng, and Y. Chen, *Phys. Rev. B* **89**, 075110 (2014).
- [11] A. Kitaev, *Ann. Phys. (Amsterdam)* **321**, 2 (2006).
- [12] H. Yao and S. A. Kivelson, *Phys. Rev. Lett.* **108**, 247206 (2012).
- [13] H. C. Jiang, Z. Y. Weng, and D. N. Sheng, *Phys. Rev. Lett.* **101**, 117203 (2008).
- [14] S. Yan, D. Huse, and S. R. White, *Science* **332**, 1173 (2011).
- [15] S. Depenbrock, I. P. McCulloch, and U. Schollwöck, *Phys. Rev. Lett.* **109**, 067201 (2012).
- [16] H. C. Jiang, Z. H. Wang, and L. Balents, *Nat. Phys.* **8**, 902 (2012).
- [17] N. Read and S. Sachdev, *Phys. Rev. Lett.* **66**, 1773 (1991).
- [18] X. G. Wen, *Phys. Rev. B* **44**, 2664 (1991).
- [19] X. G. Wen, *Phys. Rev. B* **40**, 7387 (1989).
- [20] L. Balents, M. P. A. Fisher, and C. Nayak, *Phys. Rev. B* **60**, 1654 (1999).
- [21] T. Senthil and M. P. A. Fisher, *Phys. Rev. B* **62**, 7850 (2000); *Phys. Rev. Lett.* **86**, 292 (2001).
- [22] P. Chandra and B. Douçot, *Phys. Rev. B* **38**, 9335(R) (1988).
- [23] L. B. Ioffe and A. I. Larkin, *Int. J. Mod. Phys. B* **02**, 203 (1988).
- [24] S. Sachdev and R. N. Bhatt, *Phys. Rev. B* **41**, 9323 (1990).
- [25] Andrey V. Chubukov and Th. Jolicoeur, *Phys. Rev. B* **44**, 12050(R) (1991).
- [26] M. E. Zhitomirsky and K. Ueda, *Phys. Rev. B* **54**, 9007 (1996).
- [27] A. E. Trumper, L. O. Manuel, C. J. Gazza, and H. A. Ceccatto, *Phys. Rev. Lett.* **78**, 2216 (1997).
- [28] R. R. P. Singh, Z. Weihong, C. J. Hamer, and J. Oitmaa, *Phys. Rev. B* **60**, 7278 (1999).
- [29] L. Capriotti and S. Sorella, *Phys. Rev. Lett.* **84**, 3173 (2000).
- [30] L. Capriotti, F. Becca, A. Parola, and S. Sorella, *Phys. Rev. Lett.* **87**, 097201 (2001).
- [31] G. M. Zhang, H. Hu, and L. Yu, *Phys. Rev. Lett.* **91**, 067201 (2003).
- [32] K. Takano, Y. Kito, Y. Ono, and K. Sano, *Phys. Rev. Lett.* **91**, 197202 (2003).
- [33] M. Mambrini, A. Läuchli, D. Poilblanc, and F. Mila, *Phys. Rev. B* **74**, 144422 (2006).
- [34] R. Darradi, O. Derzhko, R. Zinke, J. Schulenburg, S. E. Krüger, and J. Richter, *Phys. Rev. B* **78**, 214415 (2008).
- [35] L. Isaev, G. Ortiz, and J. Dukelsky, *Phys. Rev. B* **79**, 024409 (2009).
- [36] J. Richter and J. Schulenburg, *Eur. Phys. J. B* **73**, 117 (2010).
- [37] J. Reuther and P. Wölfle, *Phys. Rev. B* **81**, 144410 (2010).
- [38] J. F. Yu, Y. J. Kao, *Phys. Rev. B* **85**, 094407 (2012).
- [39] L. Wang, Z. C. Gu, F. Verstraete, and X. G. Wen, arXiv: 1112.3331.
- [40] H. C. Jiang, H. Yao, and L. Balents, *Phys. Rev. B* **86**, 024424 (2012).
- [41] K. S. D. Beach, *Phys. Rev. B* **79**, 224431 (2009).
- [42] F. Mezzacapo, *Phys. Rev. B* **86**, 045115 (2012).
- [43] T. Li, F. Becca, W. J. Hu, and S. Sorella, *Phys. Rev. B* **86**, 075111 (2012).
- [44] L. Wang, D. Poilblanc, Z. C. Gu, X. G. Wen, and F. Verstraete, *Phys. Rev. Lett.* **111**, 037202 (2013).
- [45] W. J. Hu, F. Becca, A. Parola, and S. Sorella, *Phys. Rev. B* **88**, 060402 (2013).
- [46] R. L. Doretto, *Phys. Rev. B* **89**, 104415 (2014).
- [47] Y. Qi and Z. C. Gu, arXiv:1308.2759 [*Phys. Rev. B* (to be published)].
- [48] A. Kitaev and J. Preskill, *Phys. Rev. Lett.* **96**, 110404 (2006).
- [49] M. Levin and X.-G. Wen, *Phys. Rev. Lett.* **96**, 110405 (2006).
- [50] R. Ganesh, J. van den Brink, and S. Nishimoto, *Phys. Rev. Lett.* **110**, 127203 (2013).
- [51] Z. Zhu, D. A. Huse, and S. R. White, *Phys. Rev. Lett.* **110**, 125205 (2013).
- [52] S. S. Gong, D. N. Sheng, O. I. Motrunich, and M. P. A. Fisher, *Phys. Rev. B* **88**, 165138 (2013).
- [53] T. Senthil, L. Balents, S. Sachdev, A. Vishwanath, and M. P. A. Fisher, *Phys. Rev. B* **70**, 144407 (2004).
- [54] T. Senthil, A. Vishwanath, L. Balents, S. Sachdev, and M. P. A. Fisher, *Science* **303**, 1490 (2004).
- [55] I. P. McCulloch and M. Gulácsi, *Europhys. Lett.* **57**, 852 (2002); I. P. McCulloch, *J. Stat. Mech.* (2007) P10014.
- [56] A. W. Sandvik, *Phys. Rev. Lett.* **98**, 227202 (2007).
- [57] R. G. Melko and R. K. Kaul, *Phys. Rev. Lett.* **100**, 017203 (2008).
- [58] F. Jiang, M. Nyfeler, S. Chandrasekharan, and U. Wiese, *J. Stat. Mech.* (2008) P02009.
- [59] J. Lou, A. W. Sandvik, and N. Kawashima, *Phys. Rev. B* **80**, 180414(R) (2009).
- [60] J. Lou and A. W. Sandvik, *Phys. Rev. B* **80**, 212406 (2009).
- [61] A. W. Sandvik, *Phys. Rev. Lett.* **104**, 177201 (2010).
- [62] M. S. Block, R. G. Melko, and R. K. Kaul, *Phys. Rev. Lett.* **111**, 137202 (2013).
- [63] S. Pujari, K. Damle, and F. Alet, *Phys. Rev. Lett.* **111**, 087203 (2013).
- [64] A. W. Sandvik, *Phys. Rev. B* **85**, 134407 (2012).
- [65] We get much better convergence on cylinder than on torus. We can achieve the truncation error  $1 \times 10^{-6}$  for  $L_y = 10$  cylinder and  $5 \times 10^{-6}$  for  $L_y = 12$  cylinder. For example, for  $J_2 = 0.5$  and  $L_y = 10$ , we get the truncation error  $1 \times 10^{-6}$  on cylinder by keeping 20000 states, while the error is much larger,  $8 \times 10^{-5}$ , on  $10 \times 10$  torus even when we keep 32000 states.
- [66] S. R. White and A. L. Chernyshev, *Phys. Rev. Lett.* **99**, 127004 (2007).
- [67] We get converged  $m_s^2$  for  $L \leq 12$  by keeping more than 20000 states, while the results for  $L = 14$  are obtained through extrapolations with the DMRG truncation error.
- [68] See Supplemental Material at <http://link.aps.org/supplemental/10.1103/PhysRevLett.113.027201> for more details.
- [69] In  $U(1)$  DMRG calculations for  $L_y \geq 10$ , one needs to extrapolate  $\xi_y$  with the DMRG truncation error, which may give some uncertainty to  $\xi_y$ .